Micro/Nanolithography, MEMS, and MOEMS

SPIEDigitalLibrary.org/jm3

Metal-organic hybrid resonant terahertz absorbers with SU-8 photoresist dielectric layer

Dragoslav Grbovic
Fabio Alves
Brian Kearney
Benjamin Waxer
Rolando Perez
George Omictin

SPIE

Metal-organic hybrid resonant terahertz absorbers with SU-8 photoresist dielectric layer

Dragoslav Grbovic
Fabio Alves
Brian Kearney
Naval Postgraduate School
Department of Physics
833 Dyer Road
Monterey, California 93943
E-mail: dgrbovic@nps.edu

Benjamin Waxer
California Institute of Technology
Pasadena, California 91106

Rolando Perez
George Omictin
Hartnell College
411 Central Avenue
Salinas, California 93901

Abstract. We report on the characterization of metal-organic hybrid metamaterials for MEMS-based terahertz (THz) thermal sensors and on the characterization of refractive index of SU-8 in the THz band. This type of metamaterial, coupled with the applicability of SU-8 as a structural material, offers possibilities for quick, simple microfabrication of THz imagers. SU-8, a negative photoresist, is a low-cost material that can quickly be spun onto a substrate at a wide range of thicknesses, and then photolithographically patterned into a variety of structures. It is also transparent to THz radiation and thus a suitable choice for a dielectric spacer in metamaterials. We investigated metamaterials consisting of a 0.18 μm Al ground plane and 0.18-μm layer of patterned Al separated by a dielectric spacer of ~0.5 μm of SU-8. Absorption close to 70% at around 6.1 THz was observed. A model was developed to simulate absorption spectra of several metamaterials, agreeing well with experiments. Matching simulation to measurements was used to determine the refractive index of SU-8 at THz frequencies, extending the known values from 0.1 to 1.6 THz to as far as 10 THz. Finally, Kirchoff's law for these metamaterials was verified and their use as THz emitters demonstrated with about 0.8 mW/cm^2 output. [DOI: 10.1117/1.JMM.12.4.041204]

Subject terms: micromachining; metamaterials; organic–inorganic hybrid materials; electromagnetic wave absorption; terahertz radiation; terahertz absorption.

Paper 13085SS received Jun. 21, 2013; revised manuscript received Aug. 19, 2013; accepted for publication Sep. 16, 2013; published online Oct. 22, 2013.

1 Introduction

Terahertz (THz) radiation is nonionizing and penetrates most nonmetallic materials. These properties make THz radiation very attractive for imaging applications in medicine[1,2] and security,[3] as it is harmless to living tissues, while able to detect metallic objects due to strong reflection. Unfortunately, background THz emission at 300 K is very small compared to shorter wavelength infrared (IR) radiation, and uncooled imaging in this spectral range has to be performed either in transmission or reflection mode using a THz illuminating source.[4] A number of different techniques have been employed to generate THz radiation[5] with varying power levels. However, the most promising devices suitable for compact imaging systems are quantum cascade lasers (QCLs).[6–8] Due to the intrinsic characteristics of QCLs, a limited amount of power output concentrated in an extremely narrow band is available. These imaging systems demand very sensitive detectors that can exhibit resonant characteristics, tuned to the laser frequency. Lately, such detectors have been demonstrated using metamaterial structures as sensitive elements.[9] Metamaterial films, which can be tuned to absorb nearly 100% of the desired THz frequency, are essentially periodic arrays of metallic elements and a conducting ground plane separated by a thin layer of dielectric material.[10,11] Dielectric layer can be used as both a structural material and dielectric spacer at the same time in MEMS focal plane arrays for THz imaging.[9] Fabrication of such sensors, using SiO_2 or SiN_x as a structural material and dielectric metamaterial layer, typically requires deposition techniques normally achieved using complex and expensive instruments. Furthermore, deposition and patterning processes for the dielectric layer can require many hours. In order to simplify and greatly reduce the deposition and patterning step times (down to minutes), we investigated the possibility of using a material suitable for quick deposition and patterning as a structural dielectric layer. SU-8 has been used in the past as a structural material for MEMS devices[12,13] and presented itself as a good choice for hybrid metal-organic THz metamaterials.

Another interesting application of the metamaterial structures is the possibility for their use as an alternative for generating THz through tailoring of a heated object's emissivity to match a specific THz frequency of interest. According to Kirchoff's law of thermal radiation, in thermodynamic equilibrium, the fraction of the incident power absorbed by the metamaterial structures should be equal to its emissivity at the same frequency.[14] In this sense, a source and sensor can be fabricated using the same process and exhibit the same spectral response, assuring optimum efficiency. The thermal generation of narrowband THz with controlled emissivity has been demonstrated in Ref. 15. In this paper, we report on the fabrication, absorption, and emission characterization of Al/SU-8/Al THz metamaterial absorbers.

The two main approaches to designing systems for THz imaging have been retrofitting of microbolometer-based IR imagers, optimized for wavelengths (8 to 12 μm),[16] and uncooled bi-material-based IR imaging technology.[17] However, both of these share the same limitation: they have low sensitivity in the THz region and do not account

for the low power output of THz sources. To overcome this limitation, several groups have been developing metamaterial films using different configurations of micro-scale metallic element arrays[18–22] that exhibit high absorption in the THz frequencies and can be integrated in microelectromechanical systems bi-material sensors.[9] Good descriptions of the physical principles behind the metamaterial absorbers can be found in Refs. 18, 19, 21, and 22. In practice, a conducting ground plane, thicker than the skin depth in the frequency of operation, prevents any transmission of the incident wave while most of the energy is reflected except at the resonance where the electromagnetic properties are such that the structure is impedance-matched with the surrounding media (free space in our case). In this situation, ideally, there is no transmission and no reflection, resulting in total absorption. By controlling the shape, thickness, and properties of metallic and dielectric layers, it is possible to tune metamaterials to the desired frequency.[10,11]

Most of the recent work on metamaterial absorbers in the 1 to 10 THz range rely on 8[23] and 4-μm[24,25] thick layers of polyimide as the dielectric spacer. Since bi-material pixel membranes are typically about 1-μm thick,[9,17] the use of 4 to 8 μm films would substantially increase thermal capacitance, negatively impacting the real-time imaging performance due to increase in the thermal time constant. Recent research on THz detectors has focused on bi-material-based imagers utilizing a thin SiO_2 and SiN_x dielectric layers and Al and Au metallic layers. Besides the difficulties in depositing SiO_2 and SiN_x films[9,26] as well as increased process times, when compared with spin-coated materials, the residual stress is very high, imposing heavy restrictions on the fabricated pixels. Therefore, considering that Hopcroft et al. has fabricated MEMS cantilevers using SU-8,[12] and many other groups have taken advantage of SU-8 as a structural material,[12,13] this material presented itself as a good alternative for THz sensors. SU-8 is attractive for its biocompatibility and its 2 to 3 GPa Young's modulus.[12] We explore the use of thin layers of SU-8 for rapid prototyping or even rapid production of metamaterials with flexible design parameters, suitable for THz bi-material sensor fabrication. For any material to be used as a structural and absorber material, optical properties (such as refractive index) in the desired band need to be available for design and optimization. This paper reports on SU-8 optical properties in the THz band.

2 Finite-Element Modeling

Finite-element (FE) modeling, using COMSOL Multiphysics software, was used to simulate absorption spectra to predict and confirm the experimental results. The method described in Refs. 10 and 11 was used to model the metamaterial films. The unit cell used in the simulations is illustrated in Fig. 1, where the dielectric layer of SU-8 is located between the 180 nm Al ground plane and an array of Al squares with the same thickness and periodicity of 21 μm. This metamaterial configuration allows the variation of the Al square dimensions to adjust the resonant frequency of the THz absorption.

The incident power is conveniently set to 1 W. Therefore, the integration of the power flow along the input port boundary gives the fraction of the power reflected (R) by the metamaterial structure. Since there is no transmission and the second-order scattering in these structures is negligible,[11] the absorption is calculated as: $A = 1 - R$. FE modeling also allows the integration of resistive heat losses in all three layers of metamaterial, which gives the absorbed fraction of the incident power directly [Fig. 1(b)]. Both methods provide identical results.

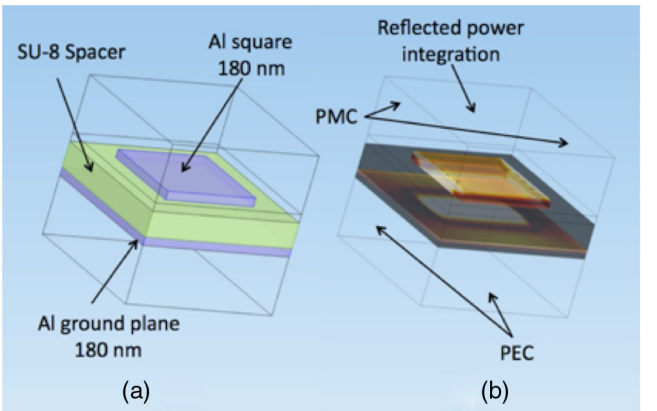

Fig. 1 (a) Simple unit cell showing bottom (uniform) and top (patterned) Al layers separated by a dielectric spacer and (b) one of the outputs of finite element (FE) model showing resistive heating (used to simulate absorption). This figure also shows that the left and right sides of the unit cell were designated as perfect magnetic conductors and the front and back sides were designated as perfect electric conductors to emulate an infinite array in the x and y-directions.

The material properties used for metal layers were: Al conductivity of 10^7 S/m measured using a four-point contact probe, after deposition of the ground plane layer. Al thickness of 180 nm for both ground plane and squares was obtained using KLA-Tencor D120 surface profilometer. SU-8 thickness of 537 nm was measured using a Filmetrics F40 spectral reflectance thickness measurement instrument. The refractive index (n) of SU-8, used for our calculation, comes from a linear extrapolation of the data reported by Arscott et al.[27] into the range of frequencies of interest (Fig. 2). A linear fit of the refractive index values for a 520-nm thick SU-8, reported in Ref. 27 in the range of 0.1 to 1.6 THz, gives: $n = -0.05\,f[\mathrm{THz}] + 1.755$. The

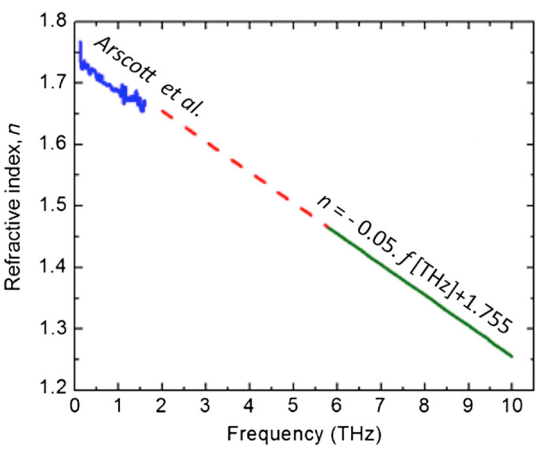

Fig. 2 Refractive index of SU-8 as a function of frequency. The 0.1–1.6 THz range was retrieved from Arscott et al. and the 5.8 to 10 THz range was estimated by linear extrapolation.

thickness used by Arscott et al. was the main reason for thickness of material used in this project.

The accuracy of this expression for frequencies in the 5.8 to 10 THz range was validated by comparing FE simulations with absorption measurements. The measured peak absorption frequencies, which are strongly dependent on the refraction index of the dielectric layer, were in good agreement with the FE simulations (Fig. 3).

3 Microfabrication

The metamaterial fabrication was simple, requiring only four processing steps. Thermal evaporation was initially used to deposit a 180-nm layer of Al to serve as the ground plane [Fig. 4(a)]. A 537-nm layer of SU-8 negative photoresist was then spun onto the sample to serve as a dielectric layer [Fig. 4(b)], softbaked for 60 s, polymerized by exposing it to the 120 mJ/cm^2 UV using Canon PLA-501S contact aligner and hard baked. SU-8 2000 0.5 was selected as it provides close to 500 nm, which we intended to use when spin coated at 3000 rpm. A coating of SPR 220 7.0 photoresist was then spun onto the SU-8 and photolithographically patterned and developed to form the metamaterial square openings. Using thermal evaporation, another 180-nm layer of Al was deposited [Fig. 4(c)]. Subsequent liftoff allowed only the metamaterial Al squares, sized between 12.1 and 14.3 μm, to remain on top of the SU-8 layer [Fig. 4(d)]. Figure 4(e) shows the optical micrograph of one of the fabricated structures. Some spots on the metal squares are present suggesting some impurities present in the top layer, most likely coming from mixing of the metal and SPR-220 photoresist during the metal evaporation step. Furthermore, the conductivity of the top Al layer was found to be two times lower than the ground plane.

4 Results

4.1 *Absorption*

The absorption in the 6 to 10 THz range for each sample was measured using a Thermo Nicolet Nexus 870 Fourier Transform Infrared Spectrometer (FTIR) spectrometer equipped with a Pike MappIR accessory, pyroelectric detector, Si beamsplitter, and globar source. The optical configuration of the FTIR ensured the area measured is around 1 cm^2, and that uniformity was such that it did not dramatically influence the absorption results. A gold mirror was used to measure the background signal. The angle of incidence was 15 deg; this was shown to produce only a minor change in the reflectance and hence did not affect the measurement significantly.[11] The absorbance was then calculated using $A = 1 - R$ and compared with simulations (Fig. 3). A detailed description of the measurement procedure is provided in Ref. 11.

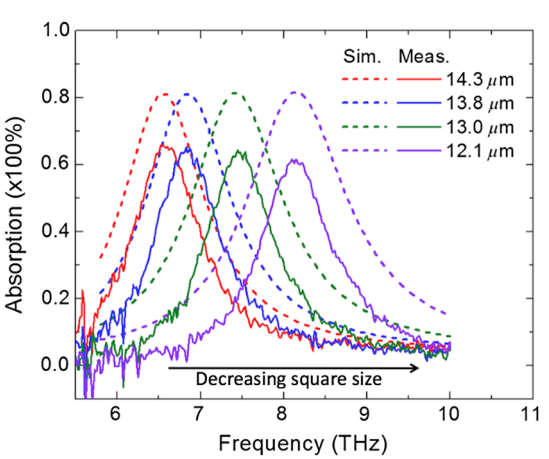

Fig. 3 Simulated (dashed) and measured (solid) absorption spectra using a linear fit obtained from a FE model where the *n* values were estimated by extrapolation from Arscott et al.

Direct measurements using the FTIR showed dips in reflection ranging from 35% to 40% at frequencies between 6.2 and 8 THz, corresponding to nearly 65% absorption for the 14.3 μm square configuration and 60% absorption for 12.1 μm square (Fig. 3). As seen in Fig. 4, assuming linear dependence of refractive index of SU-8 on frequency, the simulation accurately estimated the resonant frequencies of each film. The discrepancies in the absorption magnitude (peak heights) are most likely due to the lower conductivity of the patterned Al, probably due to contamination during the evaporation process, as well the compromised integrity of the top layers, resulting in areas of the metamaterial missing the patterned squares, effectively reducing the metamaterial fill factor, and as discussed in Ref. 11, the magnitude of the peak. Agreement of the resonant frequencies (shown to depend heavily on the value of refractive index), obtained by the FE model and FTIR measurements, verifies our extrapolation of refractive index into the 5.8 to 10 THz band. This conclusion effectively extends the range of the refractive index of SU-8 much further in the THz band.

As can be seen in Fig. 3, the absorption spectrum can be controlled by varying the dimensions of the Al squares, confirming the predictions in Ref. 11. This tunability allows the tailoring of metamaterials to the frequency of the illumination source used in a given application.

4.2 *Emission*

To verify that this metamaterial also conforms to Kirchoff's law,[14] we have measured the emission of the sample at 300°C as SU-8 has a degradation temperature of ~380°C (Ref. 28). The sample was heated on an Al-coated hot plate and the emitted radiation was redirected to the external port of our FTIR spectrometer. The Al coating exhibits very low emissivity in the THz range (Fig. 5) and greatly reduces the thermal radiation emitted by the hot plate, reducing background interference and providing a cleaner signal from the sample. An Si wafer, coated with black carbon, was used as a blackbody reference emitter. By dividing the measured metamaterial radiance by the reference radiance (at the same temperature), the emission spectra were normalized and the emissivity curves shown in Fig. 5 were obtained. It is worthwhile to note that the emissivity peaks occurred approximately at 6.4, 6.5, 7.1, and 7.8 THz for 14.3, 13.8, 13, and 12.1 μm square dimensions, respectively. The emissivity curves, measured at 300°C, show a redshift near to 0.3 THz, when compared to the peaks of the absorption curves measured at room temperature (24°C). Such a shift indicates that at 300°C there is a positive offset in the refractive index curve shown in Fig. 2. Absorption measurements were performed both before and after the emission measurements and they are identical, indicating total recovery of the metamaterial. Integration of the emissivity curves multiplied by the radiant exitance of a blackbody, at the desired temperature (shown in

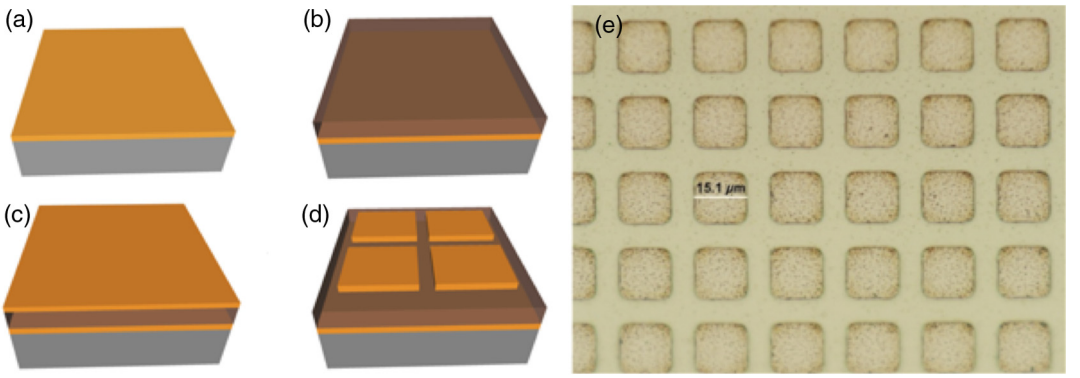

Fig. 4 Steps taken to fabricate the metamaterial: (a) deposition of 180 nm of Al via thermal evaporation, (b) addition of a 537 nm SU-8 layer via a spin coater, (c) spin-coating, patterning of SPR 220-7 photoresist followed by another deposition of 180 nm of Al, (d) liftoff of top Al layer to form metamaterial absorbers, and (e) Optical micrograph of a section of the finished metamaterial.

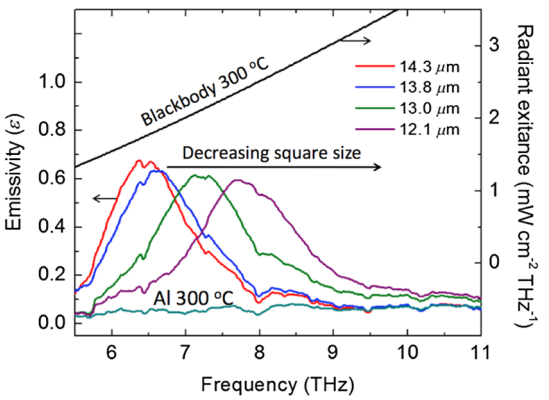

Fig. 5 Measured emissivity of the metamaterial structures at 300°C (left) and theoretical radiant exitance of a blackbody at the same temperature (right).

Fig. 5 with the vertical scale on the right for 300°C), gives the emitted power per unit area of metamaterial. For example, a back-of-the-envelope calculation for the sample with 14.3 μm can be performed as follows: Taking the half maximum width of the emissivity (~1.5 THz) and multiplying by the radiant exitance of the blackbody at the frequency of the peak emissivity (~0.8 mW/cm^2 THz^{-1}) and the peak emissivity (~0.7) gives an emitted power of 0.84 mW/cm^2. Therefore, 10 cm^2 area, of the same sample, radiates approximately 8 mW at 300°C, which is comparable to the average power emitted by a high power QCL.[7]

5 Conclusion

In summary, the absorption and emissivity of metamaterials utilizing a dielectric layer of SU-8 in the 6 to 10 THz range have been assessed via FE modeling and experimental means. The measured parameters were found to be similar to those of SiO_2-based metamaterials reported previously.[11] The structures, shown to exhibit absorption peaks >60% for a very thin layer of SU-8, can be further improved. Possible reasons for absorption peaks being lower than predicted by the model include the metallization and patterning process for the patterned layer. As seen in Fig. 3, the impurity of the metal deposition may have resulted in lower conductivity, but more importantly, damage in some of the areas where patterned structures were missing. The combination of these two factors may have caused the absorption to be lower than predicted. Replacing the liftoff by wet or dry etch patterning is expected to bring the absorption closer to the predicted values. Increasing the SU-8 thickness and improving the quality of the patterned aluminum layer could bring the absorption peak even closer to that of SiO_2. This work shows that organic epoxies, such as SU-8, are a promising choice for hybrid metamaterial structures for THz absorbers and emitters, especially in situations where rapid prototyping, large areas, and simpler means of application (such as painting) are required.

References

1. S. M. Kim et al., "Biomedical terahertz imaging with a quantum cascade laser," *Appl. Phys. Lett.* **88**(15), 153903 (2006).
2. Z. Taylor et al., "Reflective terahertz imaging of porcine skin burns," *Opt. Lett.* **33**(11), 1258–1260 (2008).
3. J. F. Federici et al., "THz imaging and sensing for security applications —explosives, weapons and drugs," *Semicond. Sci. Technol.* **20**(7), S266 (2005).
4. M. Tonouchi, "Cutting-edge terahertz technology," *Nat. Photon.* **1**(2), 97–105 (2007).
5. M. S. Shur and V. Ryzhii, "New concepts for submillimeter-wave detection and generation," in *11th GAAS Symposium*, Munich, pp. 301–304 (2003).
6. R. Kohler et al., "Terahertz semiconductor-heterostructure laser," *Nature* **417**(6885), 156–159 (2002).
7. S. Kumar, "Recent progress in terahertz quantum cascade lasers," *IEEE J. Sel. Top. Quantum Electronics* **17**(1), 38–47 (2011).
8. B. S. Williams, "Terahertz quantum-cascade lasers," *Nat. Photon.* **1**(9), 517–525 (2007).
9. F. Alves et al., "Microelectromechanical systems bimaterial terahertz sensor with integrated metamaterial absorber," *Opt. Lett.* **37**(11), 1886–1888 (2012).
10. F. Alves et al., "Strong terahertz absorption using SiO_2/Al based metamaterial structures," *Appl. Phys. Lett.* **100**(11), 111104 (2012).
11. B. Kearney et al., "Al/SiO_x/Al single and multiband metamaterial absorbers for terahertz sensor applications," *Opt. Eng.* **52**(1), 013801 (2013).
12. M. Hopcroft et al., "Micromechanical testing of SU-8 cantilevers," *Fatigue Fract. Eng. Mater. Struct.* **28**(8), 735–742 (2005).
13. H. Lorenz et al., "SU-8: a low-cost negative resist for MEMS," *J. Micromech. Microeng.* **7**(3), 121–124 (1997).
14. G. I. Kirchhoff, "On the relation between the radiating and absorbing powers of different bodies for light and heat," *Lond. Edinburgh Dublin Philos. Mag. J. Sci.* **20**(130), 1–21 (1860).
15. F. Alves et al., "Narrowband terahertz emitters using metamaterial films," *Opt. Express* **20**(19), 21025–21032 (2012).
16. B. N. Behnken et al., "Real-time imaging using a 2.8 THz quantum cascade laser and uncooled infrared microbolometer camera," *Opt. Lett.* **33**(5), 440–442 (2008).
17. D. Grbovic et al., "Arrays of SiO_2 substrate-free micromechanical uncooled infrared and terahertz detectors," *J. Appl. Phys.* **104**(5), 054508 (2008).
18. H. T. Chen, "Interference theory of metamaterial perfect absorbers," *Opt. Express* **20**(7), 7165–7172 (2012).
19. H. T. Chen et al., "Antireflection coating using metamaterials and identification of its mechanism," *Phys. Rev. Lett.* **105**(7), 73901 (2010).

20. N. Landy et al., "Perfect metamaterial absorber," *Phys. Rev. Lett.* **100** (20), 207402 (2008).
21. D. Y. Shchegolkov et al., "Perfect subwavelength fishnetlike metamaterial-based film terahertz absorbers," *Phys. Rev. B* **82**(20), 205117 (2010).
22. Q. Y. Wen et al., "Transmission line model and fields analysis of metamaterial absorber in the terahertz band," *Opt. Express* **17**(22), 20256–20265 (2009).
23. H. Tao et al., "A dual band terahertz metamaterial absorber," *J. Phys. D* **43**(22), 225102 (2010).
24. X. J. He et al., "Dual-band terahertz metamaterial absorber with polarization insensitivity and wide incident angle," *Prog. Electromag. Res.* **115**, 381–397 (2011).
25. Y. Ma et al., "A terahertz polarization insensitive dual band metamaterial absorber," *Opt. Lett.* **36**(6), 945–947 (2011).
26. H. Tao et al., "Performance enhancement of terahertz metamaterials on ultrathin substrates for sensing applications," *Appl. Phys. Lett.* **97**(26), 261909 (2010).
27. S. Arscott et al., "Terahertz time-domain spectroscopy of films fabricated from SU-8," *Electron. Lett.* **35**(3), 243–244 (1999).
28. F. Chollet Ed., "SU-8: thick photo-resist for MEMS," http://memscyclopedia.org/su8.html (7 September 2007).

Biographies and photographs of the authors are not available.